Mem. S.A.It. Vol. 90, 170

Memorie della

High-energy view of hard X-ray selected radio galaxies

F. Ursini[1], L. Bassani[1], F. Panessa[2], G. Bruni[2], A. Bazzano[2], A. J. Bird[3], A. Malizia[1], and P. Ubertini[2]

[1] INAF-Osservatorio di astrofisica e scienza dello spazio di Bologna, Via Piero Gobetti 93/3, 40129 Bologna, Italy, e-mail: `francesco.ursini@inaf.it`
[2] INAF-Istituto di Astrofisica e Planetologia Spaziali, via Fosso del Cavaliere 100, 00133 Roma, Italy
[3] School of Physics and Astronomy, University of Southampton, SO17 1BJ, UK

Abstract. We discuss results of a multiwavelength study of a sample of ∼ 70 radio galaxies, selected in the soft gamma-ray band from *INTEGRAL* and *Swift*/BAT catalogues. The sample contains a significantly larger fraction of giant radio galaxies (linear size > 0.7 Mpc) than typically found in radio surveys. These giant objects are consistent with being powered by efficient accretion, and with having experienced episodes of restarting activity. Concerning the absorption properties of the whole sample, we find a higher detection rate of 21 cm H I absorption among X-ray absorbed sources. This might suggest that at least part of the X-ray obscuration is due to atomic hydrogen seen at radio frequencies, and that could reside at distances larger than the classical pc-scale torus.

Key words. galaxies: active – galaxies: nuclei – galaxies: Seyfert – X-rays: galaxies

1. Introduction

Active galactic nuclei (AGNs) can launch powerful, radio-emitting jets, whose interaction with the surrounding medium can produce bright radio lobes, as seen in radio galaxies. The average properties of radio galaxies are generally studied in samples selected from radio catalogues. However, hard X-ray emission provides an efficient way to select nearby AGNs. Bassani et al. (2016) extracted a sample of 64 AGNs with extended radio morphology from the hard X-ray catalogues of *INTEGRAL*/IBIS (Malizia et al. 2012) and *Swift*/BAT (Baumgartner et al. 2013). Surprisingly, Bassani et al. (2016) found that this selection favours large size radio galaxies: 22% of the objects reach sizes greater than 0.7 Mpc and are classified as giant radio galaxies (GRGs). This fraction of GRGs is much larger than typically found in radio catalogues (e.g. 6% in the 3CR catalogue Ishwara-Chandra & Saikia 1999). The discovery of GRGs is difficult because of their diffuse nature and low surface brightness (Dabhade et al. 2017) and, so far, only ∼ 350 GRGs have been reported in the literature (Kuźmicz et al. 2018).

The reason for their enormous size is a matter of debate. Given their huge size, GRGs should be very old and their growth could be related to episodic activity (e.g. Subrahmanyan et al. 1996).

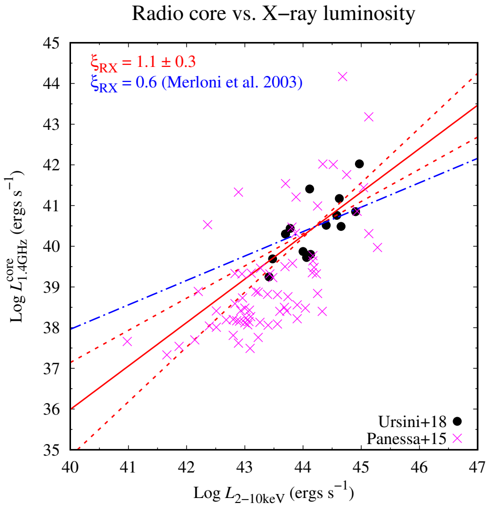

Fig. 1. Radio core 1.4-GHz luminosity versus X-ray 2–10 keV luminosity for the hard X-ray GRGs (adapted from Ursini et al. 2018b). The red solid line represents a linear fit in the log-log space, while the red dashed lines correspond to the 90 per cent error on the slope and normalization. The blue dot-dashed line represents the relation of Merloni et al. (2003) for a black hole mass of 10^8 solar masses. Black dots denote the sources of Ursini et al. (2018b). Magenta crosses denote the hard X-ray selected AGN of Panessa et al. (2015), overlayed in the plot.

Concerning the X-ray absorption properties, the column density distribution of the Bassani et al. (2016) sample is analogous to that of non-radio galaxies (Panessa et al. 2016). However, no source is found to be Compton-thick and, in general, so far we lack strong evidence for heavily absorbed radio galaxies Ursini et al. (2018a).

2. Giant radio galaxies

2.1. Radio core–X-ray relation

The radio core luminosity, the X-ray luminosity and the black hole mass of AGNs and black hole X-ray binaries are related via the so-called fundamental plane of black hole activity (Merloni et al. 2003).

In fig. 1 we plot the radio core luminosity $L^{\rm core}_{\rm 1.4GHz}$ against the X-ray luminosity $L_{\rm 2-10keV}$, for both the GRGs analysed in Ursini et al. (2018b) and a complete sample of hard X-ray selected AGNs (Panessa et al. 2015), together with the relation of Merloni et al. (2003). The hard X-ray GRGs follow the steep correlation ($\xi_{\rm RX} \simeq 1$) typical of hard X-ray AGNs. This is consistent with the 'efficient' branch of the fundamental plane, which is physically interpreted as a signature of a radiatively efficient accretion flow (Coriat et al. 2011; Gallo et al. 2012).

2.2. Bolometric luminosity and jet power

We computed two independent estimates of the bolometric luminosity, from the luminosity of the radio lobes ($L^{\rm radio}_{\rm bol}$) and from the X-ray luminosity ($L^{\rm X}_{\rm bol}$). To compute $L^{\rm radio}_{\rm bol}$, we used a correlation between the 1.4-GHz luminosity of the radio lobes and the bolometric luminosity estimated from the optical one (van Velzen et al. 2015). To compute $L^{\rm X}_{\rm bol}$, we used the 2–10 keV bolometric correction of Marconi et al. (2004). We plot the two estimates in Fig. 2 (left panel). At least in 9 objects out of 14, $L^{\rm radio}_{\rm bol}$ is around one order of magnitude smaller than $L^{\rm X}_{\rm bol}$. This in turn suggests that either their nuclear luminosity is higher than the average luminosity during their lifetime, or that their lobes luminosity is lower than expected (possibly due to radiative losses).

We also estimated the time-averaged kinetic power of the jet from the extended radio luminosity, using the relationship reported by Willott et al. (1999). In Fig. 2 (right panel) we plot the bolometric luminosity $L^{\rm X}_{\rm bol}$ against the jet power Q_j, for both the hard X-ray GRGs and the sample of bright (> 2 Jy) radio galaxies of Mingo et al. (2014). Hard X-ray GRGs have X-ray-derived bolometric luminosities similar to those of high-excitation radio galaxies (broad/narrow-line radio galaxies and quasars) in the Mingo et al. (2014) sample. On the other hand, their estimated jet powers are much lower. A tentative interpretation is that GRGs could begin their life with high nuclear luminosities/high jet powers and move to lower luminosities in time. If the central engine gradually fades (and eventually switches

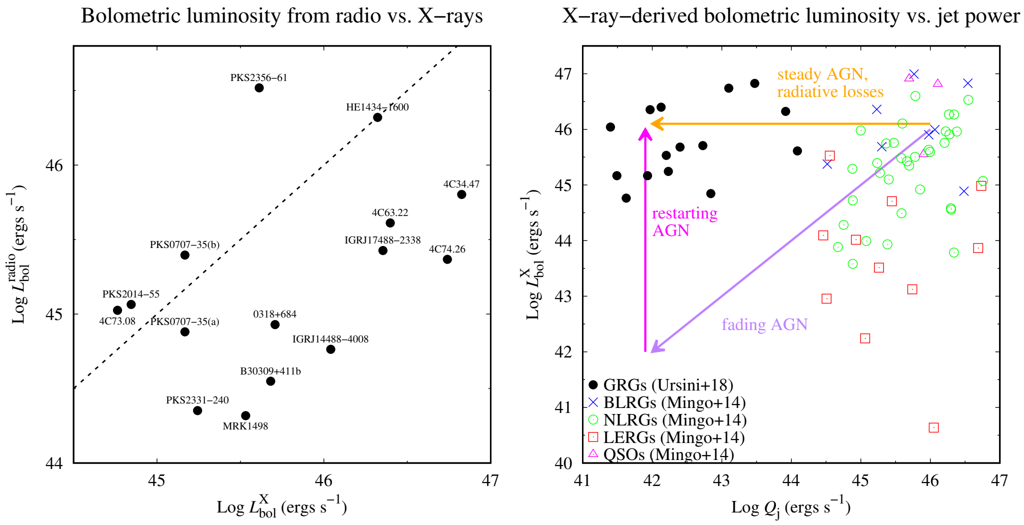

Fig. 2. Left panel: Bolometric luminosity estimated from the radio luminosity of the lobes (y-axis) versus that estimated from the 2–10 keV luminosity (x-axis) for the hard X-ray GRGs (Ursini et al. 2018b). The dashed line represents the identity $y = x$. Right panel: Bolometric luminosity estimated from the 2–10 keV luminosity versus jet power estimated from the relation of Willott et al. (1999) (adapted from Ursini et al. 2018b). Black dots denote the hard X-ray GRGs, while coloured symbols denote the radio bright sources of Mingo et al. (2014). Coloured arrows denote possible evolutionary tracks.

off), most of radio-selected GRGs would have low nuclear luminosities. Hard X-ray selection instead picks GRGs with a high nuclear luminosity, i.e. those that either kept a constant nuclear power during their life or that experienced episodes of restarting activity. The latter scenario is favoured by the discovery of a large fraction (60%) of young radio cores (Bruni et al. 2019) and by the radio morphological properties (Bruni et al., in preparation).

3. Multiwavelength absorption properties

The circumnuclear hydrogen gas in radio galaxies can be traced by both 21 cm H I absorption and soft X-ray absorption. Recently, a correlation was found between the 21 cm H I column density ($N_{\mathrm{H\,I}}$) and the X-ray hydrogen column density ($N_{\mathrm{H,X}}$), suggesting a link between the two gas populations (Moss et al. 2017; Ostorero et al. 2017). Among the hard X-ray radio galaxies of Bassani et al. (2016), 26 have been observed at 21 cm and H I absorption was detected in 7 cases (Fig. 3, left panel). Interestingly, the detection rate is much higher among X-ray absorbed sources (6/10). This might indicate a common origin for both radio and X-ray absorption, either from a pc-scale torus or galactic-scale material. The largest X-ray column density is found in NGC 612, which is surrounded by a 140 kpc-wide disc of neutral hydrogen (Emonts et al. 2008).

Concerning the infrared absorption, the strength of the silicate feature at 9.7 μm, $S = \ln(F(\lambda_{\mathrm{peak}})/F_c(\lambda_{\mathrm{peak}}))$, is a diagnostic for dusty torus models. When the absorption features is deep ($S < -1$), it cannot be entirely explained by dusty torus models and rather indicates a contamination from obscuration in the host galaxy (e.g. Goulding et al. 2012). Among the hard X-ray radio galaxies, sources with silicate absorption are X-ray obscured and detected at 21 cm (Fig. 3, right panel). The deepest silicate absorption is found in NGC 612, suggesting that galactic-scale obscuration could have a significant impact.

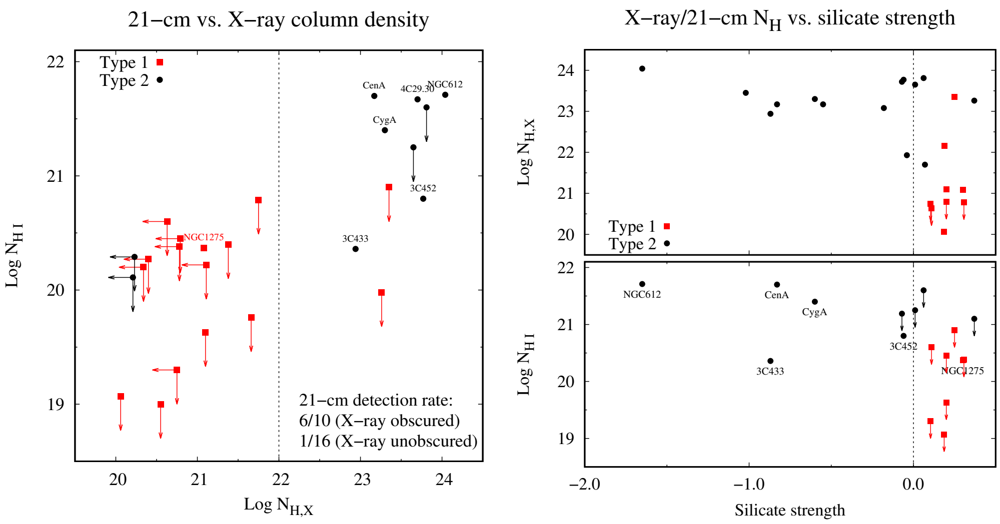

Fig. 3. Left panel: 21 cm H I column density versus total hydrogen column density constrained from X-rays for the sample of Bassani et al. (2016). Black dots denote optical type 2 sources; red squares denote optical type 1 sources. Arrows represent upper limits. Sources with $N_{\mathrm{H,X}} > 10^{22}$ cm^{-2} are considered as X-ray absorbed. Right panel: 21 cm H I column density (top) and X-ray column density (bottom) versus the strength of the silicate feature at 9.7 μm.

Acknowledgements. We acknowledge financial support from ASI and INAF under INTEGRAL "accordo ASI/INAF 2013-025-R1".

References

Bassani, L., Venturi, T., Molina, M., et al. 2016, MNRAS, 461, 3165

Baumgartner, W. H., Tueller, J., Markwardt, C. B., et al. 2013, ApJS, 207, 19

Bruni, G., Panessa, F., Bassani, L., et al. 2019, ApJ, 875, 88

Coriat, M., Corbel, S., Prat, L., et al. 2011, MNRAS, 414, 677

Dabhade, P., Gaikwad, M., Bagchi, J., et al. 2017, MNRAS, 469, 2886

Emonts, B. H. C., Morganti, R., Oosterloo, T. A., et al. 2008, MNRAS, 387, 197

Gallo, E., Miller, B. P., & Fender, R. 2012, MNRAS, 423, 590

Goulding, A. D., Alexander, D. M., Bauer, F. E., et al. 2012, ApJ, 755, 5

Ishwara-Chandra, C. H. & Saikia, D. J. 1999, MNRAS, 309, 100

Kuźmicz, A., et al. 2018, ApJS, 238, 9

Malizia, A., Bassani, L., Bazzano, A., et al. 2012, MNRAS, 426, 1750

Marconi, A., Risaliti, G., Gilli, R., et al. 2004, MNRAS, 351, 169

Merloni, A., Heinz, S., & di Matteo, T. 2003, MNRAS, 345, 1057

Mingo, B., Hardcastle, M. J., Croston, J. H., et al. 2014, MNRAS, 440, 269

Moss, V. A., Allison, J. R., Sadler, E. M., et al. 2017, MNRAS, 471, 2952

Ostorero, L., Morganti, R., Diaferio, A., et al. 2017, ApJ, 849, 34

Panessa, F., Bassani, L., Landi, R., et al. 2016, MNRAS, 461, 3153

Panessa, F., Tarchi, A., Castangia, P., et al. 2015, MNRAS, 447, 1289

Subrahmanyan, R., Saripalli, L., & Hunstead, R. W. 1996, MNRAS, 279, 257

Ursini, F., Bassani, L., Panessa, F., et al. 2018a, MNRAS, 474, 5684

Ursini, F., Bassani, L., Panessa, F., et al. 2018b, MNRAS, 481, 4250

van Velzen, S., Falcke, H., & Körding, E. 2015, MNRAS, 446, 2985

Willott, C. J., et al. 1999, MNRAS, 309, 1017